Activation-Induced Subcellular Redistribution of $G\alpha_s$ Is Dependent upon Its Unique N-Terminus†

Manimekalai M. Thiyagarajan,‡ Eve Bigras,§ Hubert H. M. Van Tol,|| Terence E. Hébert,§ Daniel S. Evanko,‡,⊥ and Philip B. Wedegaertner*,‡

Department of Microbiology and Immunology, Kimmel Cancer Center, Thomas Jefferson University, Philadelphia, Pennsylvania 19107, Centre de Recherche, Institut de Cardiologie de Montréal, 5000 Bélanger est, Montréal, Quebec, Canada H1T 1C8, and Laboratory for Molecular Neurobiology, Centre for Addiction and Mental Health, 250 College Street, Toronto, Ontario, Canada M5T 1R8

Received January 10, 2002; Revised Manuscript Received April 23, 2002

ABSTRACT: The heterotrimeric G protein subunit, α_s, can move reversibly from plasma membranes to cytoplasm in response to activation by GPCRs or activating mutations. We examined the importance of the unique N-terminus of α_s in this translocation in cultured cells. α_s contains a single site for palmitoylation in its N-terminus, and this was replaced by different plasma membrane targeting motifs. These N-terminal α_s mutants were targeted properly to plasma membranes, capable of coupling activated GPCRs to effectors, and able to constitutively stimulate cAMP production when they also contained an activating mutation. However, when activated by a constitutively activating mutation or by agonist-activated β-AR, these N-terminal α_s mutants failed, for the most part, to undergo redistribution from plasma membranes to cytoplasm, as assayed by immunofluorescence microscopy, or from a particulate to soluble fraction, as assayed by subcellular fractionation. These results highlight the importance of the extreme N-terminus of α_s and its single site of palmitoylation for facilitating activation-induced translocation and provide insight into the mechanism of this G protein trafficking event.

Many proteins require association with the plasma membrane (PM) for proper functioning, and in many cases, membrane localization of signaling proteins is regulated and reversible. The heterotrimeric ($\alpha\beta\gamma$) G proteins[1] are typically found at the PM where they interact with receptors and effectors. Binding of the α subunit to the $\beta\gamma$ dimer is critical for its proper targeting to the PM (*1*−*5*). However, when the heterotrimer is activated and the α and $\beta\gamma$ subunits dissociate, the α subunit must rely on its intrinsic membrane binding ability to remain associated with the PM.

All $G\alpha$ subunits are acylated at the N-terminus by the fatty acids myristate and/or palmitate, and these modifications are required for proper membrane localization (*6*−*8*). Myristate provides only low-affinity binding to membranes (*9*). Therefore, other mechanisms of membrane binding, such as positive charges or protein−protein interactions, would be required to efficiently anchor myristoylated proteins to membranes (*10*). On the other hand, palmitate has sufficient binding energy to stably anchor a protein to membranes (*7*). With the exception of α_t, all G protein α subunits contain palmitate (16-carbon, saturated fatty acid) attached through labile, reversible thioester linkages to one or more cysteines at the amino terminus (*11*). Palmitoylation, due to its reversibility, thus provides the potential to be an important mechanism for regulating a protein's attachment to membranes. Indeed, several G protein α subunits undergo more rapid depalmitoylation upon activation by an appropriate G protein-coupled receptor (GPCR) (*12*−*16*). Furthermore, at least one G protein α subunit, α_s, undergoes rapid activation-induced subcellular redistribution. α_s can translocate from the PM to the cytoplasm upon receptor triggered activation, mutational activation, or cholera toxin-mediated activation (*17*−*22*). The redistribution of α_s in response to the β-adrenergic receptor (β-AR) agonist, isoproterenol, is rapid (about 10 min) and is reversible by the β-AR antagonist, propanolol (*18*). When activated by β-AR, redistributed α_s does not appear to colocalize with internalized receptors, nor does its redistribution require endocytosis of the β-AR, suggesting that redistribution of α_s is independent of GPCR trafficking.

Translocation of α_s from PM to cytoplasm correlates with demonstrations of activation-induced depalmitoylation of α_s (*12*−*14*). However, the importance of depalmitoylation in the observed activation-induced cytoplasmic shift of α_s remains to be defined. Inhibitors or activators of the depalmitoylation reaction have not been identified. For other G protein α subunits, much less evidence is available to support activation-induced changes in subcellular localiza-

† Supported by National Institutes of Health Grant GM56444 (P.W.) and the Pew Scholars Program in the Biomedical Sciences (P.W.).

* To whom correspondence should be addressed. Phone: 215-503-3137. Fax: 215-923-2117. E-mail: P_Wedegaertner@mail.jci.tju.edu.

‡ Thomas Jefferson University.

§ Centre de Recherche, Institut de Cardiologie de Montréal.

|| Laboratory for Molecular Neurobiology, Centre for Addiction and Mental Health.

⊥ Present address: Department of Neuroscience, University of Pennsylvania, 215 Stemmler Hall, Philadelphia, PA 19104.

[1] Abbreviations: G protein, heterotrimeric guanine nucleotide binding regulatory protein; wt, wild type; PAGE, polyacrylamide gel electrophoresis; SDS, sodium dodecyl sulfate; GPCR, G protein-coupled receptor; DMEM, Dulbecco's modified Eagle medium; PM, plasma membrane; DAR-1, *Caenorhabditis elegans* dopamine receptor 1.

10.1021/bi025533u CCC: $22.00
Published on Web 06/27/2002

tion. The N-termini of G protein α subunits are quite diverse in terms of amino acid sequence and combinations of lipid modifications. Most α subunits are modified by two lipids, either two palmitates or myristate plus palmitate; α_s appears to contain only one attached palmitate. Thus, the presence of only one site of reversible palmitoylation in α_s may underlie the reversible membrane localization of α_s. In this model (*11*), rapid removal of the single palmitate from the N-terminus of α_s would allow it to translocate off of the PM.

To address the importance of the unique N-terminus of α_s in activation-induced subcellular redistribution, we constructed several N-terminal mutants of α_s. In these mutant proteins, the extreme N-terminus of α_s, which contains the cysteine site of palmitoylation, was replaced by a variety of potential membrane targeting motifs. We examined the effect of these N-terminal changes on the activation-induced redistribution of α_s. The results demonstrate that mutant α_s subunits containing alternative N-terminal plasma membrane targeting motifs fail to translocate from the plasma membrane to cytoplasm in response to activation.

EXPERIMENTAL PROCEDURES

Materials. HEK293 cells were obtained from the American Type Culture Collection (CRL-1573). [2-^{3}H]Adenine was from Amersham Pharmacia Biotech. [9,10-^{3}H]Palmitic acid and [9,10-^{3}H]myristic acid were from Perkin-Elmer Life Science Products. 12CA5 monoclonal antibody was from Roche Molecular Biochemicals, EE mouse monoclonal antibody was a gift from Dr. Henry Bourne (UCSF), and the β-AR polyclonal antiserum was a gift of Dr. Mark von Zastrow (UCSF). Tissue culture reagents were from Mediatech and Life Technologies, Inc. Other reagents were from Fisher Scientific and Sigma Biochemical Co.

Plasmid Constructions. HA-α_s and HA-α_q in pcDNA3 or pcDNAI, containing the internal HA epitope sequence (DVPDYA), have been described (*1*, *23*). EE-α_{i2}-pcDNAI, containing an internal EE epitope (EEYMPTE), has also been used previously (*24*). N-Terminal mutants of α_s were constructed by PCR mutagenesis, using the following 5′ mutagenic primers: 5′gcggcgtcgaccatgggctgcctaggcagtagtaagaccgaggaccag3′ (α_sN6S); 5′gcggcgtcgaccatgggctgcacctaagtagtaagaccgaggaccag3′ (myr$^+$/palm$^+$ α_s); 5′gcggcgtcgaccatgggatccaccttaagtagtaagaccgaggaccag3′ (myr$^+$/palm$^-$ α_s); 5′ggctagcgatatcatggggagtagcaagagcaagcctaaggaccccagccagcgccggcgtaaggcgcagcgcgaggcc3′ (myr$^+$/polybasic α_s); 5′gcggcgatatccatgactctggagtccatcatggcatgctgcctcggcaacagtaagaccg3′ (2palm α_s); 5′ggctagcgatatcatggcgcccaagaaagggctgctccagagactcttcaagcggcagcatcagaacaattccaagagtaaggcgcagcgcgaggcc3′ (polybasic α_s). SP6 primer was used as the 3′ primer. For myr$^+$/polybasic α_s, 2palm α_s, and polybasic α_s, PCR products were digested with *Eco*RV and *Xho*I and ligated with HA-α_s pcDNA3 vector cut with *Eco*RV and *Xho*I. The R201C activating mutation was introduced into myr$^+$/polybasic α_s, 2palm α_s, and polybasic α_s constructs by ligating an *Eco*NI−*Xho*I fragment excised from HA-α_s-RC pcDNA3 into appropriately digested α_s amino-terminal mutants. For α_sN6S, myr$^+$/palm$^+$ α_s, and myr$^+$/palm$^-$ α_s, PCR products were digested with *Sal*I and *Eco*RI and ligated with HA-α_s-pcDNAI vector cut with *Sal*I and *Eco*RI. The RC activating mutation was introduced into α_sN6S myr$^+$/palm$^+$ α_s and myr$^+$/palm$^-$ α_s constructs by ligating an *Eco*RI−*Bgl*II fragment excised from the mutants into appropriately digested HA-α_s-RC pcDNAI. The resulting constructs were verified by DNA sequencing (Kimmel Cancer Center Nucleic Acids Facility) to contain no mutations other than those desired. Human β_1-pCMV5 and bovine γ_2-pcDNAI have been described (*25*).

Cell Culture and Transfection. HEK293 cells were maintained in DMEM containing 10% fetal bovine serum and gentamicin as described previously (*2*). Transfections were carried out with 1 μg of total plasmid DNA in six-well cell culture plates or 3 μg of total plasmid DNA in 6 cm plates using FuGENE 6 Transfection Reagent (Roche Molecular Biochemicals) according to the manufacturer's instructions. Cells were transfected overnight, transferred to new plates the next day, and grown for 24−30 h prior to subsequent manipulations.

Metabolic Labeling and Immunoprecipitation. Radiolabeling of α_s and the mutants with fatty acids was performed essentially as described previously (*1*). Briefly, 48 h after transfection COS cells in a 6 cm dish were incubated with 1 mL of media containing [9,10-^{3}H]palmitic acid (1 mCi) or [9,10-^{3}H]myristic acid (0.25 mCi) for 4 h. Cells were washed once with PBS and lysed (50 mM HEPES, pH 7.4, 150 mM NaCl, 0.5% sodium deoxycholate, 1% NP-40, 1 mM EDTA, 2.5 mM $MgCl_2$, 1 mM PMSF, 2 μg/mL leupeptin, 2 μg/mL aprotinin), and the extracts were tumbled for 1 h at 4 °C. Nuclei and insoluble material were removed by centrifugation. 12CA5 antibody was added, and samples were tumbled for 2 h at 4 °C. Twenty microliters of Protein A/G Plus agarose (Santa Cruz Biotechnology, Santa Cruz, CA) was added, and samples were then tumbled overnight at 4 °C. The beads were pelleted by centrifugation at 200*g* and washed with lysis buffer, and SDS−PAGE sample buffer was added. Samples were heated to 65 °C for 1 min. An aliquot was then fractionated by 10% SDS−PAGE. The SDS−PAGE gel was soaked for 20 min each in 50% methanol/10% acetic acid, 10% methanol/10% acetic acid, and Amplify (Amersham Pharmacia Biotech). Gels were then dried and subjected to fluorography at −80 °C using Hyperfilm MP (Amersham Pharmacia Biotech). Bands were photographed using a Kodak DC40 imaging system, and images were processed using Adobe Photoshop and Canvas[7] SE version 8.6.

Subcellular Fractionation. Soluble and particulate fractions were isolated as previously described (*2*). Briefly, HEK293 cells were transfected with the indicated amounts of each expression plasmid in 6 cm plates. Twenty-four hours after transfection, the cells were transferred to 10 cm plates and grown for 48 h. Cells were washed with phosphate-buffered saline and then lysed in 0.5 mL of hypotonic lysis buffer by 10 passages through a 27-gauge needle. Cells were centrifuged to pellet nuclei and intact cells, and the supernatant was centrifuged at 150000*g* to obtain soluble and particulate fractions. Fractions were resolved by 10% SDS−PAGE, transferred onto PVDF-Plus (Micron Separations, Inc.), and probed with 12CA5 or EE monoclonal antibody. Bands were visualized by chemiluminescence and quantitated using a Kodak DC40 imaging system. Graphs were prepared using GraphPad Prism version 3.0a.

Immunofluorescence Microscopy. Immunofluorescence localization was performed as described previously (*2*).

Briefly, HEK293 cells were transfected with the indicated amounts of each expression plasmid. Twenty-four hours after transfection in six-well plates, cells were replated on glass coverslips and grown for 24−48 h. In some experiments cells were treated in the absence and presence of 10 μM β-AR agonist isoproterenol at 37 °C. Cells expressing HA-α_s, HA-α_s mutants, or HA-α_q were then fixed with 3.7% formaldehyde in phosphate-buffered saline (PBS) for 15 min. Cells expressing EE-α_{i2} were fixed in methanol at −20 °C for 20 min. Coverslips were incubated in blocking buffer (2.5% nonfat milk and 1% Triton X-100 in PBS) for 30 min. Samples were then incubated with 12CA5 (3 μg/mL) and/or β-AR-specific rabbit polyclonal antiserum (1:1000 dilution) (*18*) or EE (20 μg/mL) mouse monoclonal antibodies in blocking buffer for 1 h. The cells were washed with blocking buffer and incubated in a 1:100 dilution of Alexa 594 goat anti-mouse and/or Alexa 488 goat anti-rabbit (Molecular Probes, Eugene, OR) secondary antibodies for 30 min. The coverslips were washed with 1% Triton X-100 in PBS, rinsed in distilled water, and mounted on glass slides with 10 μL of Prolong Antifade reagent (Molecular Probes, Eugene, OR). Microscopy was performed with an Olympus BX60 microscope with a Sony DKC-5000 digital camera and images processed with Adobe Photoshop. Transfections were repeated at least three times, and hundreds of cells were examined for each construct. Representative pictures were taken of cells displaying low to intermediate levels of expression.

Subcellular localization of each expressed α subunit was determined and quantitated in terms of the number of cells displaying a particular subcellular localization phenotype. Three independent observers who were blinded to the identity of the expressed α subunit analyzed at least 150 cells. Only cells displaying low levels of expression were counted. Cells were monitored by taking images with the CCD camera to ensure that cells being counted all gave a visible but not saturated image at identical exposure times. Subcellular localization of each counted cell was classified as one of three phenotypes: (1) predominantly PM; (2) combination of PM and cytoplasm; or (3) cytoplasm only. Predominant PM localization was defined as bright staining at a cell's periphery and lacking a visible negatively stained nucleus or nuclear shadow. A combination of PM and cytoplasm staining (PM/cytoplasm) was defined as some degree of visible sharp staining at a cell's periphery and the presence of a nuclear shadow. Such a nuclear shadow is consistent with cytoplasmic and/or intracellular membrane localization, since staining in areas surrounding the nucleus typically produces the appearance of a dark nucleus in these experiments. Cytoplasmic only localization was defined as no visible staining at a cell's periphery, diffuse staining throughout the cell's interior, and the presence of a nuclear shadow. The number of cells displaying each localization phenotype was expressed as a percentage of the total along with 95% confidence interval (CI). Statistical analysis of the data was performed using a two-sample binomial proportion test (*26*).

Confocal Microscopy. Coverslips were prepared for confocal microscopy exactly as described above under Immunofluorescence Microscopy. Representative images were recorded at the Kimmel Cancer Center Confocal Microscopy Facility using a Bio-Rad MRC-600 laser scanning confocal microscope running CoMos 7.0a software and interfaced to a Zeiss Axiovert 100 microscope with Zeiss Plan-Apo 63 × 1.40 NA oil immersion objective. All α subunit images were recorded at identical gain and black level settings to ensure that all analyzed cells were expressing similar low levels of the α subunit. All α subunit samples were analyzed using excitation at 568 nm, while dual-labeled samples were analyzed using simultaneous excitation at 488 and 568 nm. Images of "*x*−*y*" sections through the middle of a cell were recorded.

Quantitation of confocal microscopy images of single cells was performed using the Plot Profile tool of NIH ImageJ software. The relative magnitude of α subunit distribution along a linear slice of the cell was quantitated, similar to that described previously (*27*). The average pixel intensity in 8−15 traces from $n \geq 5$ cells for each α subunit was determined and plotted. Gray values of the distribution curves were normalized to 100. Histograms of wild type versus RC activated or wild type versus isoproterenol activated are presented together to reveal quantitative differences in plasma membrane localization.

cAMP Assays. cAMP production was measured as described previously (*1*). For measurements of α_{2A}-adrenergic receptor-dependent cAMP accumulation, 24 h after transfection HEK293 cells were reseeded into six wells of a 24-well plate to provide three samples for basal cAMP determination and three samples for agonist-stimulated cAMP determination. [2-^{3}H]Adenine (2 μCi/mL) was added to the each. All cells were grown for another 24 h. The cells were washed with 0.5 mL of prewarmed wash buffer and then incubated in wash media with 1 mM IBMX with or without 10 μM UK-14304 for 45 min at 37 °C. The reactions were terminated by lysing the cells in ice-cold 5% TCA containing 1 mM cAMP and 1 mM ATP. [^{3}H]cAMP and [^{3}H]ATP were separated on AG 50w-X4 Dowex and alumina columns as described (*23*). The activity was defined as the average of ([^{3}H]cAMP)/([^{3}H]cAMP + [^{3}H]ATP) from triplicate samples. For measurements of constitutive cAMP stimulation by α_s mutants containing the R201C mutation, 24 h after transfection HEK293 cells were reseeded into two sets of triplicates in separate 24-well plates to provide three samples for cAMP determination and three samples for determining protein expression levels. cAMP production was measured in one set of samples as described above. For determination of protein expression, cells were washed with ice-cold PBS and then lysed in 0.4 mL of SDS−PAGE sample buffer per well. Samples were harvested by scraping with a pipet tip and repeated pipeting and boiled for 5 min. Ten percent of each sample was resolved by 12% SDS−PAGE, transferred to PVDF-Plus (Micron Separations, Inc.), and probed with 12CA5 monoclonal antibody. Bands were visualized by chemiluminescence and quantitated using a Kodak DC40 imaging system. Thus, the protein level in each experiment was determined to be the average intensity of three measurements. Graphs were prepared using GraphPad Prism version 3.0a.

Because of variability in levels of expressed protein upon transfection of equal amounts of DNA for each mutant, all activity was expressed relative to level of protein expression. To determine the correct amount of DNA to transfect such that we were in the linear range of protein expression and activity, we transfected increasing concentrations of DNA

for each of the α_sRC constructs and assayed the cAMP production as above. Two hundred nanograms of DNA was determined to be in the linear range when activity was plotted versus DNA concentration.

To verify that expressing the activity relative to protein levels resulted in increased accuracy, the variability of the raw activity numbers was compared to the variability in activity determined by dividing calculated activity by expressed protein. Variability was determined by calculating the coefficient of variation [(standard deviation/average) × 100] for each expressed construct. Dividing calculated activity by expressed protein resulted in a 48−90% decrease in the coefficient of variation compared to uncorrected activity for each of the expressed constructs. Therefore, correcting for the level of expressed protein resulted in a significant increase in accuracy of the measurements.

cRNA Synthesis and Electrophysiology. Xenopus oocytes were isolated as described (*28*, *29*). cDNA constructs were linearized by restriction enzymes and purified using Geneclean (Bio 101). Capped cRNA for the *Caenorhabditis elegans* dopamine receptor *dar-1*,[2] human Kir 3.2, and the various α_s subunits were made using T7 RNA polymerase or SP6 RNA polymerase. mRNA synthesis for channel, receptor, or G protein constructs was confirmed by loading aliquots of synthesis reactions on denaturing formaldehyde−agarose gels. Individual oocytes were injected with 5−10 ng (in 50 nL) of various constructs either singly or in combination. Total cRNA concentration was kept constant between injections. Currents were recorded 48−72 h after injection. Standard recording solution was KD-98 (98 mM KCl, 1 mM $MgCl_2$, 5 mM K-HEPES, pH 7.5) unless otherwise stated. Microelectrodes were filled with 3 M KCl and had resistances of 1−3 MΩ and 0.1−0.5 MΩ for voltage and current electrodes, respectively. In addition, current electrodes were back-filled with 1% agarose (in 3 M KCl) to prevent leakage as described (*28*). Recordings were made at room temperature using a Geneclamp 500 amplifier (Axon Instruments). Oocytes were voltage clamped and perfused continuously with different recording solutions. Currents were evoked by 500 ms voltage commands from a holding potential of −10 mV, delivered in 20 mV increments from −140 to 60 mV to test for inward rectifying potassium currents. Data were recorded at a holding potential of −80 mV, and drugs were added at the indicated concentrations to the bath with a fast perfusion system. Data collection and analysis were performed using pCLAMP v6.0 (Axon Instruments) and Origin v5.0 (MicroCal) software. For subtraction of endogenous and leak currents, records were obtained in ND-96 (96 mM NaCl, 2 mM KCl, 1 mM $MgCl_2$, 5 mM Na-HEPES, pH 7.5), and these were subtracted from recordings in KD-98 before further analysis.

RESULTS

Subcellular Localization of Wild Type and Mutationally Activated α *Subunits.* Most heterotrimeric G proteins are primarily associated with the plasma membrane. Immunofluorescence microscopy was utilized to examine the subcellular distribution of α_s, α_i, or α_q in their inactivated and activated states (Figure 1A). Images of representative cells are presented in Figure 1A, and quantitation based on observations of many cells is provided in Table 1. When cells were transiently transfected with epitope-tagged, wild-type forms of α_s, α_i, or α_q, each α subunit was detected predominantly at cellular plasma membranes, as seen by the bright staining at the periphery of cells (Figure 1A1, 1A3, 1A5 and Table 1). To examine the effect of activation on each of the G proteins, the cells were transiently transfected with the same α subunits containing an arginine to cysteine (RC) constitutively activating mutation. As expected, the α_s-RC subunit displayed a diffuse distribution throughout the cytoplasm with only faint staining at the PM (Figure 1A2

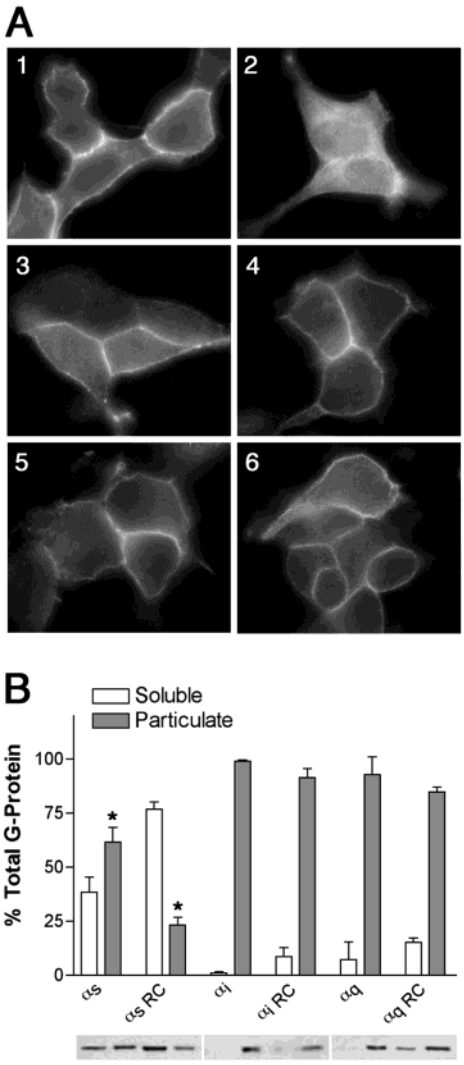

FIGURE 1: Immunofluoresence microscopy and subcellular fractionation of wild-type and mutationally activated α_s, α_i, and α_q. (A) HEK293 cells were transiently transfected with 1 μg of wild-type α_s (1), α_sRC (2), wild-type α_i (3), α_iRC (4), wild-type α_q (5), or α_qRC (6). Cells were fixed, and α subunits were visualized by indirect immunofluorescence with 12CA5 (1, 2, 5, and 6) or EE (3, 4) antibodies followed by secondary antibodies, as detailed under Experimental Procedures. (B) HEK293 cells were transiently transfected as in (A). Soluble and particulate fractions were isolated as described under Experimental Procedures. The results shown are the means ± SD for $n = 3-5$ experiments. Asterisks indicate statistical difference between wild-type and RC-activated α subunits in amount in the particulate fraction (*t*-test; $p < 0.001$). A representative western blot is shown with the bands corresponding to the columns in the graph immediately above.

[2] S. Sanyal, R. F. Wintle, E. Bigras, D. Merz, T. E. Hébert, J. G. Culotti, and H. H. M. Van Tol, manuscript in preparation.

Table 1: Quantitation of Immunofluorescence Microscopy of Wild-Type and Mutationally Activated α Subunits[a]

	PM % (95% CI)	PM/cytoplasm % (95% CI)	cytoplasm % (95% CI)
α_s[b]	87.1 (77.8, 96.4)	12.9 (3.6, 22.2)	0 (0, 0)
α_sRC[b]	4.1 (0, 9.6)	58.7 (45.1, 72.4)	37.2 (23.8, 50.6)
α_q[c]	93.0 (85.9, 100)	7.0 (0, 14.1)	0 (0, 0)
α_qRC[c]	70.2 (57.5, 82.9)	23.3 (11.6, 35.0)	6.5 (0, 13.3)
α_i	95.9 (90.4, 100)	4.1 (0, 9.6)	0 (0, 0)
α_iRC	94.7 (88.5, 100)	5.3 (0, 11.5)	0 (0, 0)
2palm α_s	92.2 (84.8, 99.6)	7.8 (0.4, 15.2)	0 (0, 0)
2palm α_sRC	74.4 (62.3, 86.5)	22.0 (10.5, 33.5)	3.5 (0, 8.6)
myr$^+$/palm$^+$ α_s	98.1 (94.3, 100)	1.9 (0, 5.7)	0 (0, 0)
myr$^+$/palm$^+$ α_sRC	98.7 (95.6, 100)	1.3 (0, 4.4)	0 (0, 0)
myr$^+$/palm$^-$ α_s[c]	7.2 (0, 14.4)	53.6 (39.8, 67.4)	39.2 (25.7, 52.7)
myr$^+$/palm$^-$ α_sRC[c]	0 (0, 0)	27.5 (15.1, 39.9)	72.5 (60.1, 84.9)
myr$^+$/polybasic α_s	88.4 (79.5, 97.3)	11.6 (2.7, 20.5)	0 (0, 0)
myr$^+$/polybasic α_sRC	81.5 (70.7, 92.3)	18.5 (7.7, 29.3)	0 (0, 0)
polybasic α_s	81.3 (70.5, 92.1)	17.3 (6.8, 27.8)	1.3 (0, 4.4)
polybasic α_sRC	91.4 (83.6, 99.2)	7.9 (0.4, 15.4)	0.7 (0, 3.0)

[a] The indicated subunits were expressed in HEK293 cells, and subcellular localization was determined using immunofluorescence microscopy. As described further under Experimental Procedures, the subcellular localization pattern of the expressed α subunit was defined as predominantly plasma membrane (PM), plasma membrane and cytoplasm (PM/cytoplasm), or cytoplasm with no detectable plasma membrane staining (cytoplasm). Approximately 150 cells were examined in each case, and the percentage of cells displaying each subcellular localization along with the 95% confidence interval (CI) is indicated in the table. [b] Significant difference in plasma membrane localization between α_s and α_sRC ($p < 0.01$; two-sample binomial proportion test). [c] Significant difference in plasma membrane localization between α_q and α_qRC and between myr$^+$/palm$^-$ α_s and myr$^+$/palm$^-$ α_sRC ($p < 0.05$; two-sample binomial proportion test).

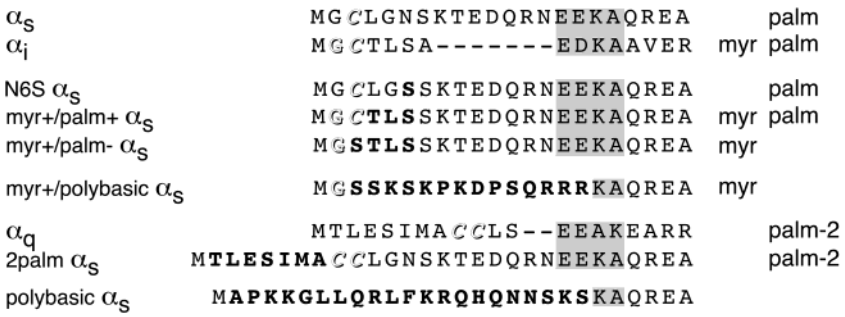

FIGURE 2: N-terminal sequences of α_s mutants. The N-terminal sequences of α_s, α_i, and α_q and N-terminal α_s mutants are shown. Sites of G protein lipid modification are indicated. Myristoylated glycines are indicated in outline format. Palmitoylated cysteines are indicated in italic outline. Conserved residues between different α subunits are shaded. Amino acid changes introduced into α_s to create the N-terminal mutants are shown in bold. The lipid modification status is indicated at the right.

and Table 1) (*18*). However, examination of activated α_iRC (Figure 1A4) showed pronounced plasma membrane staining, and there appeared to be no change in localization compared to the unactivated α_i (Table 1). α_qRC displayed mostly strong staining at the cell periphery (Figure 1A6) consistent with plasma membrane localization, but in addition, a small but significant decrease in plasma membrane localization compared to α_q was observed (Table 1). Therefore, of the three α subunits examined only α_s appears to undergo dramatic activation-induced redistribution, while α_q displays a lesser ability to redistribute upon activation, consistent with a previous report (*30*).

Activation-dependent localization of these three G proteins was also examined by cell fractionation. Consistent with the immunofluorescence microscopy results, activated α_sRC displayed a significant decrease in membrane localization, as assessed by appearance in a particulate fraction, compared to unactivated α_s while there was no significant difference between activated and unactivated α_i and α_q (Figure 1B). The acylation state of the G proteins is a potential candidate for the differential results of activation on PM localization. α_s is singly modified by palmitate and is known to be depalmitoylated in the RC activating mutant (*14*). However, α_i is both myristoylated and palmitoylated, while α_q is dually modified with two molecules of palmitate (Figure 2). We sought to determine whether these differences have any role in the observed difference in their localization upon activation.

N-Terminal Mutants of α_s *with Different PM Localization Motifs.* To address the importance of the N-terminus of α_s in its activation-induced subcellular redistribution, we constructed mutants of α_s designed to replace the single cysteine site of palmitoylation with alternative membrane targeting motifs. Initially, we sought to create an α_s similar to the α_i family that is modified by both myristate and palmitate. Although α_s contains a glycine immediately after the initiating methionine amino acid, this glycine is not a substrate for myristoylation, presumably because other N-terminal amino acids prevent proper recognition by an N-terminal myristoyl transferase (*6*). To try to produce a mutant α_s that would be palmitoylated and myristoylated, we mutated the asparagine at position 6 to serine (Figure 2) in order to reproduce the highly conserved serine present in approximately 75% of myristoylated proteins (*10*). Surprisingly, this α_sN6S mutant was not found to be myristoylated, though it did retain its ability to be palmitoylated (Figure

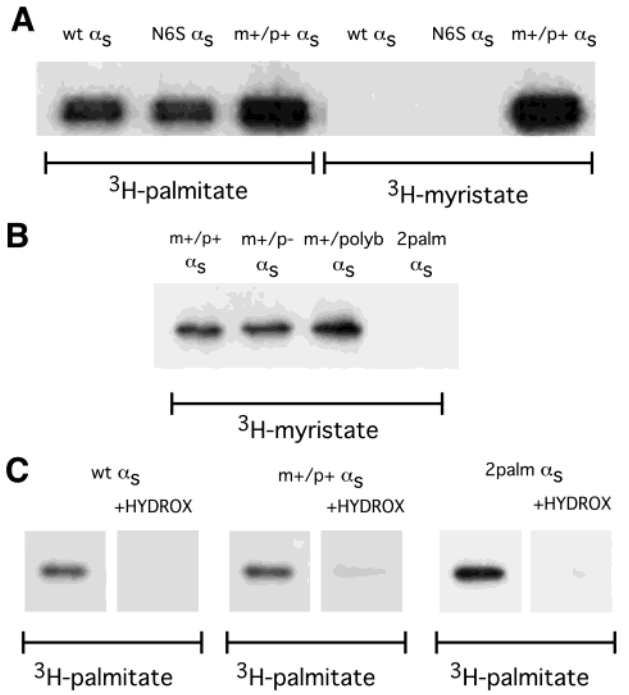

FIGURE 3: Palmitoylation and myristoylation of α_s mutants. COS cells were transiently transfected with 3 μg of α_s or the indicated α_s mutants. Later (48 h) they were incubated with 1 mCi/mL [^{3}H]-palmitic acid or 0.25 mCi/mL [^{3}H]myristic acid for 4 h. The cells were lysed, and α_s proteins were immunoprecipitated with the 12CA5 antibody. Proteins were subjected to SDS−PAGE and visualized by fluorography. (A) Palmitoylation and myristoylation were determined for wild-type α_s, N6S α_s, and myr$^+$/palm$^+$ (m+/p+) α_s. Although the α_s bands appear to be doublets in this experiment, this was not reproduced in other experiments (e.g., B and C, below) and may represent an artifact of gel drying and fluorography rather than two forms of expressed α_s. (B) The myristoylation status was compared for myr$^+$/palm$^+$ (m+/p+), myr$^+$/palm$^-$ (m+/p-), myr$^+$/polybasic (m+/polyb), and 2palm mutants. (C) After [^{3}H]palmitic acid labeling, immunoprecipitation, and SDS−PAGE, identical gels were incubated in the absence or presence (+HYDROX) of 1 M hydroxylamine, pH 7. The sensitivty to hydroxylamine treatment is shown for palmitate attached to wild-type α_s, myr$^+$/palm$^+$ (m+/p+), and 2palm mutants.

3A). Since the single mutation was not sufficient for myristoylation, we created a second mutant, myr$^+$/palm$^+$ α_s, in which residues 4 through 6 of α_s were replaced with the corresponding residues from α_i (Figure 2). Metabolic labeling indicated that these additional changes were sufficient to induce myristoylation of α_s while retaining palmitoylation (Figure 3A), as is seen in the α_i family members. Myr$^+$/palm$^+$ α_s incorporated more radiolabeled palmitate relative to wild-type α_s (Figure 3A). This observation is consistent with tighter membrane association of myr$^+$/palm$^+$ α_s compared to wild-type α_s (compare Figure 1B and Figure 4) and may reflect a higher stoichiometry of palmitoylation of myr$^+$/palm$^+$ α_s. The myr$^+$/palm$^-$ α_s mutant was constructed by introducing the well-characterized C3S mutation (*18*, *23*) in the myr$^+$/palm$^+$ mutant. As expected, myr$^+$/palm$^-$ α_s was found to be myristoylated (Figure 3B) but not palmitoylated (not shown) since the cysteine required for palmitoylation had been removed. In order to have a mutant of α_s that is myristoylated but contains an N-terminal sequence differing from that found in Gα proteins, we replaced the first 16 amino acids of α_s with amino acids 1−16 from the Src protein to create the myr$^+$/polybasic α_s mutant (Figure 2). This N-terminal region of the Src protein is myristoylated and also contains basic residues found to be important in membrane binding (*31*, *32*). Furthermore, these first 16 residues of Src were previously found to be sufficient to target GFP to the PM (*33*). We confirmed that myr$^+$/polybasic α_s does incorporate myristate as expected (Figure 3B). To examine the effect of two palmitates, a 2palm α_s mutant was designed which replaced the first three amino acids of α_s with the first 10 amino acids of α_q (Figure 2). Metabolic labeling showed that this mutant does efficiently incorporate palmitate (Figure 3C) but not myristate (Figure 3B). Since the sequence was taken directly from α_q, it is presumed that both cysteines are capable of being palmitoylated, as suggested for α_q (*23*, *34*, *35*). This is supported by the observation that the intensity of the signal observed for 2palm α_s is stronger than that observed for all of the proteins containing only one known site of palmitoylation (Figure 3C). The 2palm mutant was also analyzed by treatment with hydroxylamine, a reagent that has been demonstrated to cleave thioester-linked palmitate from cysteine residues. Treatment with hydroxylamine resulted in loss of labeling of the 2palm α_s mutant whereas the labeling in a control gel treated with Tris buffer was not lost. This confirms that the labeling is due to palmitoylation of cysteine residues (Figure 3C). Likewise, radiolabeled palmitate incorporated into wt α_s or myr$^+$/palm$^+$ α_s was sensitive to hydroxylamine (Figure 3C).

The last mutant, polybasic α_s, was designed to target α_s to plasma membranes in the absence of any lipid modifications. Amino acids 546−565 of G protein-coupled receptor kinase 5 (GRK5) comprise a polybasic region that is required for plasma membrane localization of GRK5 (*36*), and this sequence is sufficient to target GFP to the plasma membrane (A. Pronin and J. Benovic, unpublished observation). The polybasic α_s mutant was created by replacing the first 16 residues of α_s with this polybasic stretch of 20 amino acids from GRK5, thus creating a mutant α_s that should be targeted to the PM in the absence of myristoylation or palmitoylation (Figure 2). To study the subcellular localization and signaling functions of the numerous mutants of α_s (Figure 2) in both wild-type and RC-activated forms, we focused on transient expression of the subunits in HEK293 cells.

Subcellular Localization of α_s Mutants and Effect of the RC Mutation. To examine the subcellular localization of α_s and the α_s mutants containing the RC constitutively activating mutation, the G proteins were transiently transfected in HEK293 cells, and the cells were lysed and fractionated into soluble (cytosolic) and particulate (membrane) fractions. The comparison of constructs with and without the RC mutation was used as a measure of change in localization based on activation. Consistent with previous results demonstrating an activation-induced redistribution of α_s from membrane to cytosol (*18*), the majority (60%) of wild-type α_s was found in the particulate fraction while only 25% of the α_sRC mutant remained in the particulate fraction (Figure 1B). The myr$^+$/palm$^+$, myr$^+$/polybasic, and polybasic α_s mutants were observed to be strongly associated with the particulate fraction (84−98% membrane fraction) and did not undergo any significant shift upon introduction of the RC activating mutation (Figure 4). In contrast, the myr$^+$/palm$^-$ α_s mutant was observed to have greatly reduced localization to the particulate fraction (approximately 58%), consistent with

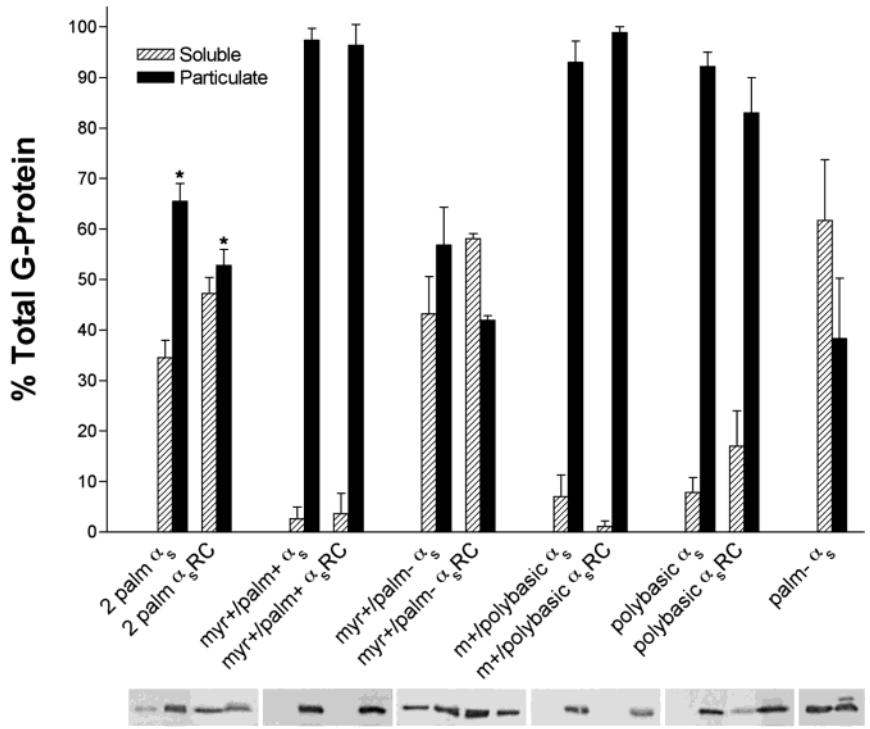

FIGURE 4: Localization of N-terminal mutants of α_s by cell fractionation. HEK293 cells were transfected with 3 μg of each mutant, either unactivated or containing the RC mutation. The cells were grown for 48 h, and the proteins were fractionated into particulate and soluble fractions as decribed in Experimental Procedures. Mutant α_s proteins in each fraction were visualized by SDS−PAGE followed by western blotting with 12CA5 antibody. The bands were quantitated and are represented as a percent of total detected soluble and particulate α_s. The results shown are the means ± SD for $n = 5-8$ experiments. Asterisks indicate statistical difference between wild-type and RC-activated α subunits in amount in the particulate fraction (*t*-test; $p < 0.01$). A representative western blot is shown with the bands corresponding to the columns in the graph immediately above.

other reports of myr$^+$/palm$^-$ mutant α subunits of the α_i family (*37*). When the RC activating mutation was added to myr$^+$/palm$^-$ α_s, a small shift to cytosolic localization was observed with approximately 45% found in the particulate fraction. Interestingly, the retention of myr$^+$/palm$^+$ α_sRC in the particulate fraction, rather than showing a more soluble fractionation similar to myr$^+$/palm$^-$ α_sRC, suggests that this mutant is not significantly in the depalmitoylated form. On the other hand, others have demonstrated that α_i undergoes receptor-activated depalmitoylation, but receptor activation does not promote increased solubility of α_i (*16*). The 2palm α_s was the only other subunit to show a change upon mutational activation with 70% of the unactivated protein particulate but only 53% of the activated protein present in the particulate fraction. The nonpalmitoylated α_s (C3S) mutant was found to be mostly (60%) in the cytosol, as described previously (*23*), and likewise, mutationally activated α_sC3S,RC is predominantly soluble (not shown). Thus, these subcellular fractionation results suggest that the alternative amino-terminal membrane targeting motifs completely abolish or hinder, in the case of myr$^+$/palm$^-$ and 2palm α_s, activation-induced redistribution of α_s.

To extend the fractionation results, we determined the subcellular localization of α_sRC mutants by performing immunofluorescence microscopy (Table 1) and confocal microscopy (Figure 5) on cells transiently transfected with each G protein α subunit construct. As previously observed, the wild-type α_s was located predominately at the plasma membrane, while α_sRC was mostly cytoplasmic (Figure 1A1, 1A2, Table 1, and Figure 5A). To further confirm the localization of wild-type α_s and α_sRC, each was colocalized with plasma membrane localized GRK5 (*36*) or cytoplasmic GRK2 (*38*) using quantitative analysis of confocal microscopy (Supporting Information). Plasma membrane localization displayed sharp peaks at the extremities of the distribution graphs while cytoplasmic localization was evidenced by the absence of peaks (whole cell staining) or wide peaks (cytoplasmic and nonnuclear staining) (distribution plots, Figure 5, and Supporting Information). Most of the unactivated mutants displayed predominant plasma membrane localization (Figure 5B,C,E,F and Table 1) which was indistinguishable from wt α_s (Figure 5A and Table 1). However, myr$^+$/palm$^-$ α_s appeared to bind to all cellular membranes indiscriminately (Figure 5D), as was previously demonstrated for α_z containing the C3S mutation to prevent palmitoylation (*39*). Inclusion of the RC activating mutation in each mutant had variable effects on localization for each mutant. The 2palm α_sRC mutant retained mostly plasma membrane staining (Figure 5B), but there appeared to be a slight increase in cytoplasmic staining, based on quantitation of many cells (Table 1), although this was variable from cell to cell. The myr$^+$/palm$^+$ α_sRC mutant (Figure 5C and Table 1) and myr$^+$/polybasic α_sRC mutant (Figure 5E and Table 1) displayed strong PM staining; thus, these two mutants were unaffected by inclusion of the activating mutation. The myr$^+$/palm$^-$ α_sRC mutant displayed mostly a staining pattern consistent with nonspecific membrane staining (Figure 5D), and in addition, a small decrease was observed in the low level of plasma membrane staining relative to unactivated myr$^+$/palm$^-$ α_s (Table 1). The polybasic α_sRC mutant remained at the PM (Figure 5F and Table 1) and, additionally, displayed some nuclear staining that was observed to a

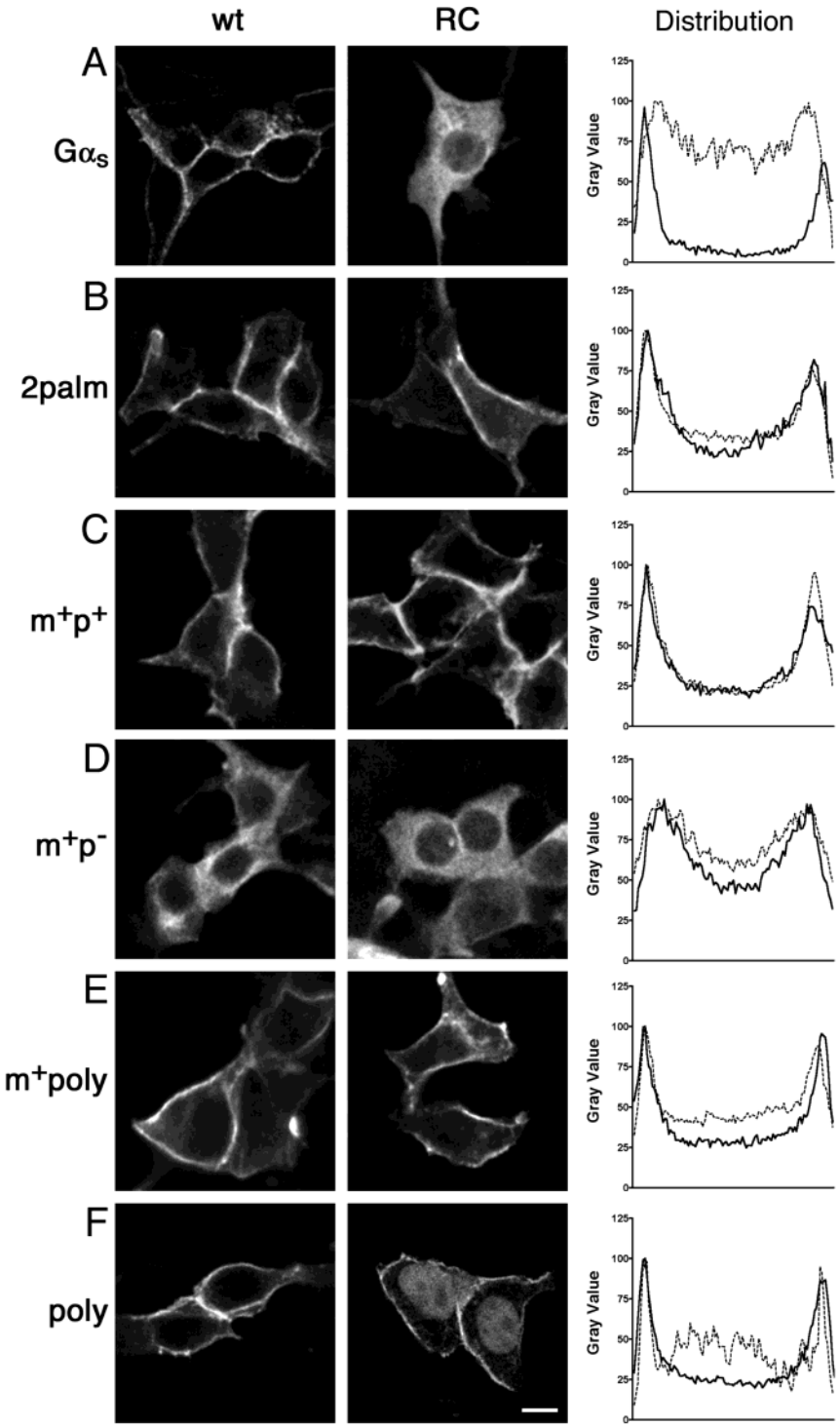

FIGURE 5: Subcellular localization of N-terminal mutants of α_s by confocal immunofluorescence microscopy. HEK293 cells were transfected with 1 μg of various α_s mutants, either unactivated or containing the RC mutation, grown for 48 h, and fixed with 3.7% formaldehyde. Cells were permeabilized and incubated with 12CA5 antibody and Alexa 594 conjugated anti-mouse antibody, and images were recorded using a confocal laser scanning microscope as described under Experimental Procedures. Representative images are shown of unactivated (left panel) or RC-activated (middle panel) α_s (A), 2palm α_s (B), myr$^+$/palm$^+$ α_s (C), myr$^+$/palm$^-$ α_s (D), myr$^+$/polybasic α_s (E), and polybasic α_s (F). Bar = 10 μm. The right panel (distribution) shows the relative average magnitudes of the unactivated (solid line) or RC-activated (broken line) α subunit concentration along linear slices of images from single cells. The traces shown represent the average pixel intensity in 8−15 traces from $n \geq 5$ cells for each α subunit. The sharp peaks at either end of a histogram trace correspond to plasma membrane localization, while an increase in magnitude of the central portion of the trace reflects increased staining in the cell's interior (i.e., localization to cytoplasm and/or intracellular membranes). Note that in the traces for α_sRC forms (A, broken line) and both forms of myr$^+$/palm$^-$ (D) a central "dip" in the plot is found corresponding to the lack of the α subunits in the nucleus. For polybasic α_sRC (F, broken line) a central "bump" in the plot is found corresponding to the partial nuclear localization of this α subunit.

lesser extent with the unactivated form (Figure 5F). Furthermore, the differences and similarities between wild-type and RC-activated α_s subunits, as described above, were readily defined and quantitated by analyses of pixel intensity across linear slices of single cells (Figure 5, distribution plots). The large difference seen in the distribution plots in

Table 2: Quantitation of Immunofluorescence Microscopy of Isoproterenol-Induced Redistribution of α Subunits[a]

	PM % (95% CI)	PM/cytoplasm % (95% CI)	cytoplasm % (95% CI)
α_s[b]	98.0 (94.1, 100)	2.0 (0, 5.9)	0 (0, 0)
α_s + iso[b]	0.65 (0, 2.9)	44.8. (31.0, 58.6)	54.5 (40.7, 68.4)
2palm α_s	96.9 (92.0, 100)	3.1 (0, 8.0)	0 (0, 0)
2palm α_s + iso	95.5 (89.7, 100)	4.5 (0, 10.3)	0 (0, 0)
myr$^+$/palm$^+$ α_s	92.4 (85.1, 99.8)	7.6 (0.2, 14.9)	0 (0, 0)
myr$^+$/palm$^+$ α_s + iso	82.1 (71.5, 92.7)	16.6 (6.3, 26.9)	1.3 (0, 4.5)
myr$^+$/palm$^-$ α_s[b]	14.1 (4.5, 23.7)	73.7 (61.5, 85.9)	12.2 (3.1, 21.2)
myr$^+$/palm$^-$ α_s + iso[b]	0 (0, 0)	10.9 (2.2, 19.5)	89.1 (80.5, 97.8)
myr$^+$/polybasic α_s	96.6 (91.5, 100)	3.4 (0, 8.5)	0 (0, 0)
myr$^+$/polybasic α_s + iso	83.0 (72.6, 93.4)	17.0 (6.6, 27.4)	0 (0, 0)
polybasic α_s[b]	90.5 (82.4, 98.6)	9.5 (1.4, 17.6)	0 (0, 0)
polybasic α_s + iso[b]	65.7 (52.5, 78.8)	30.9 (18.1, 43.7)	3.4 (0, 8.5)

[a] The indicated α subunits, along with $\beta\gamma$ and β_2-AR, were expressed in HEK293 cells. Cells on coverslips were incubated in the absence or presence of 10 μM isoproterenol (+iso) for 20 min, and subcellular localization was determined using immunofluorescence microscopy. As described further under Experimental Procedures, the subcellular localization pattern of the expressed α subunit was defined as predominantly plasma membrane (PM), plasma membrane and cytoplasm (PM/cytoplasm), or cytoplasm with no detectable plasma membrane staining (cytoplasm). Approximately 150 cells were examined in each case, and the percentage of cells displaying each subcellular localization along with the 95% confidence interval (CI) is indicated in the table. [b] Significant difference in plasma membrane localization between basal and isoproterenol-stimulated α subunits ($p < 0.01$; two-sample binomial proportion test).

Figure 5A clearly shows the difference in subcellular distribution of α_s versus α_sRC. Note that α_s, and most of the other α_s mutants, show a plot with a concave central portion and sharp peaks at either end, which is indicative of plasma membrane localization. On the other hand, a plot of α_sRC distribution (Figure 5A) shows the wider peaks and/or higher intensity in the central portion typical of cytoplasmic localization. Other plasma membrane localized α_s mutants show little or no change in the distribution plots upon RC activation (Figure 5). Thus, these conventional and confocal immunofluorescence results suggest that, in most cases, the alternative N-terminal membrane targeting motifs were effective in preventing the RC mutation-induced shift of α_s to the cytoplasm.

Localization of α_s N-Terminal Mutants upon Agonist Stimulation. Previous results utilizing cells stably transfected with α_s and/or β_2-adrenergic receptor (β_2-AR) have demonstrated that addition of the β_2-AR agonist isoproterenol causes a reversible redistribution of α_s from plasma membrane to cytoplasm (*18*). To allow a more rapid analysis of α_s mutants, we have now developed a transient transfection system to visualize β_2-AR-induced redistribution of α_s. When HEK293 cells were cotransfected with β_2-AR, Gα_s, Gβ_1, and Gγ_2, the addition of isoproterenol promoted a redistribution of α_s from plasma membrane to cytoplasm as observed by both conventional (Table 2) and confocal (Figure 6A) immunofluorescence microscopy. In addition, the β_2-AR underwent well-described (*40*, *41*) internalization via endocytic vesicles as seen by punctate cytoplasmic staining (Figure 6A). Using this transient transfection system, we assayed the ability of the amino-terminal α_s mutants to translocate from the plasma membrane to the cytoplasm upon β_2-AR activation. β_2-AR localized to plasma membranes in the basal state and efficiently internalized in response to isoproterenol when coexpressed with each α_s mutant (not shown). The 2palm α_s mutant (Figure 6B), the myr$^+$/palm$^+$ α_s mutant (Figure 6C), the myr$^+$/polybasic α_s mutant (Figure 6E), and the polybasic α_s mutant (Figure 6F) showed no change in plasma membrane staining upon addition of agonist as determined by confocal microscopy. Furthermore, these differences and similarities between wild-type and β_2-AR-activated α_s subunits were readily defined and quantitated by analyses of pixel intensity across linear slices of single cells (Figure 6, distribution plots). As described above in Figure 5 for the comparison of α_s versus α_sRC, only α_s showed a dramatic change in the shape of the distribution plot (Figure 6A, distribution plot) upon activation by isoproterenol-stimulated β_2-AR. Likewise, quantitation by immunofluorescence microscopy of populations of expressing cells (Table 2) supported the confocal microscopy results (Figure 6), with the exception of polybasic α_s which showed a small decrease in plasma membrane localization after isoproterenol treatment (Table 2). Last, unactivated myr$^+$/palm$^-$ α_s shows weak plasma membrane localization, but β_2-AR activation decreases its plasma membrane localization further (Figure 6D and Table 2). Subcellular fractionation into particulate and soluble portions was not used for the analysis of receptor-stimulated redistribution of α_s. Previous results demonstrated small and variable increases of α_s in the soluble fraction after β_2-AR activation (*14*, *17*); thus, in this case, subcellular fractionation was not a robust assay for analyzing loss of translocation by the N-terminal α_s mutants. In summary, conventional and confocal immunofluorescence microscopy revealed that the N-terminal mutants of α_s, with the exception of myr$^+$/palm$^-$ α_s, are defective in their ability to undergo β_2-AR-stimulated dissociation from plasma membranes.

Signaling Ability of α_s N-Terminal Mutants. The ability of α_s and the α_s mutants to couple an activated GPCR to effector was assayed in two ways. First, a *Xenopus* oocyte system was used to demonstrate the ability of N-terminal α_s mutants to couple to an activated GPCR. We have demonstrated previously that coexpression of a number of G_i-coupled receptors including M2 muscarinic receptors and $GABA_B$ receptors with Kir 3.2 in *Xenopus* oocytes leads to channel activation after receptor stimulation (*42*). A number of Gα_s-coupled receptors can regulate Kir 3.2 channels in oocytes when coexpressed with mammalian α_s (*29*, *43*). This obligate requirement for α_s renders these receptors an excellent system for comparing α_s mutants. We have used a *C. elegans* Gα_s -coupled receptor DAR-1,[2] which, like the β_2-AR, requires α_s for functional coupling to Kir 3.2 channels in oocytes. However, unlike the β_2-AR, the coupling of

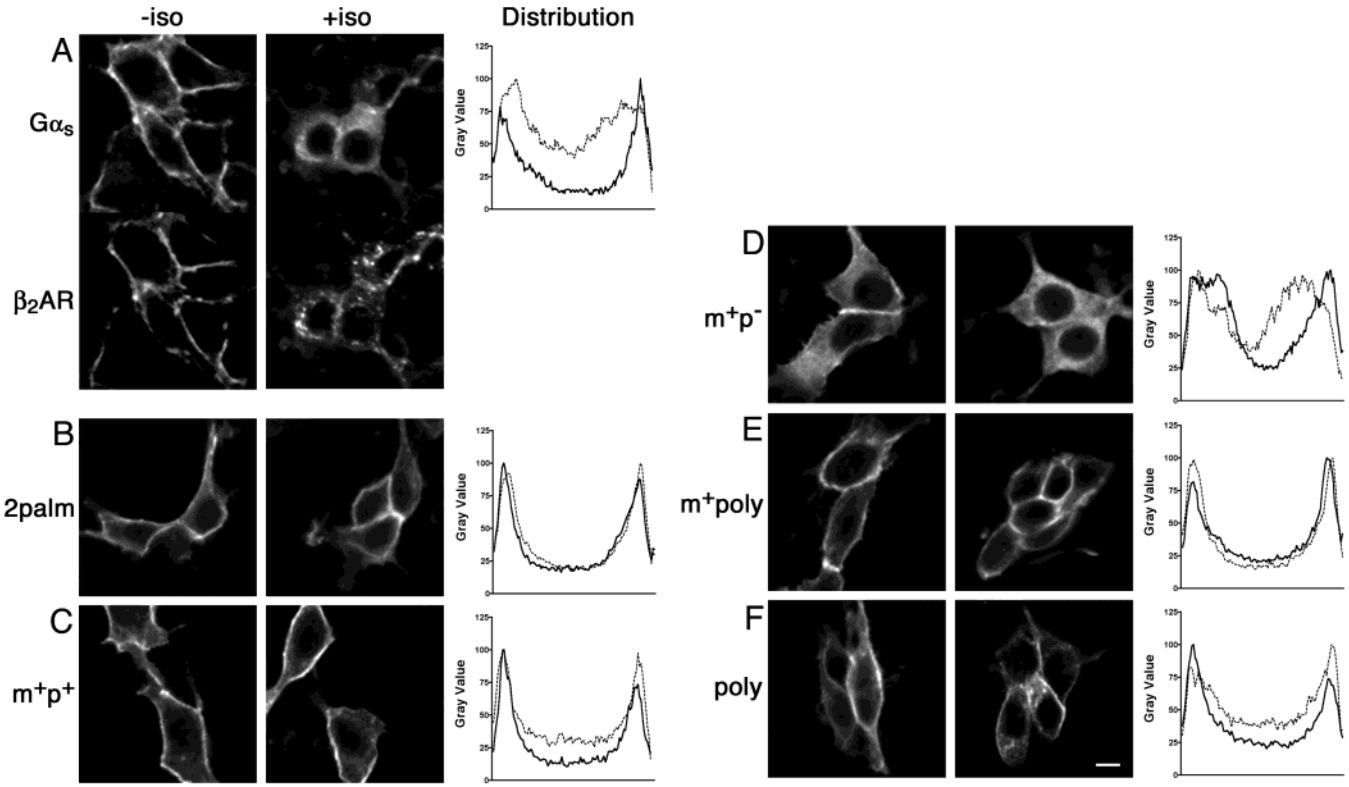

FIGURE 6: Confocal microscopy of α_s subunits after β_2-AR activation. For these experiments, HEK293 cells were transfected with 350 ng of β_2-AR, 350 ng of the indicated HA epitope-tagged α_s, 200 ng of β_1, and 100 ng of γ_2. Cells were incubated for 20 min in the absence (−iso) or presence (+iso) of 10 μM isoproterenol. Cells were fixed and processed for immunofluorescence of β_2-AR and α_s as detailed under Experimental Procedures. β_2-AR was detected using a rabbit polyclonal antibody followed by Alexa 488 conjugated anti-rabbit antibody, and α_s was detected by 12CA5 mouse monoclonal antibody followed by Alexa 594 conjugated anti-mouse antibody. Representative images are shown of unactivated (left panel) or isoproterenol-stimulated (middle panel) α_s (A), 2palm α_s (B), myr$^+$/palm$^+$ α_s (C), myr$^+$/palm$^-$ α_s (D), myr$^+$/polybasic α_s (E), and polybasic α_s (F). Colocalization of β_2-AR with wt α_s is also presented in panel A. Bar = 10 μm. The right panel (distribution) shows the relative magnitudes of the unactivated (solid line) or isoproterenol-activated (broken line) α subunit concentration along linear slices of images from single cells. The traces shown represent the average pixel intensity in 8−15 traces from $n \geq 5$ cells for each α subunit. The sharp peaks at either end of a histogram trace correspond to plasma membrane localization, while an increase in magnitude of the central portion of the trace reflects increased staining in the cell's interior (i.e., localization to cytoplasm and/or intracellular membranes). Note that in the traces for α_s +iso (A, broken line) and myr$^+$/palm$^-$ with and without iso (D) a central "dip" in the plot is found corresponding to the lack of the α subunits in the nucleus.

DAR-1 to endogenous G protein $\beta\gamma$ subunits is not variable, and thus this receptor does not require coexpression of mammalian G$\beta\gamma$ subunits as does the β_2-AR for maximal coupling (*29*). In this system, channel activation is mediated by released endogenous G$\beta\gamma$ subunits. When expressed with wild-type α_s, stimulation with 1 μM dopamine caused a robust 368 ± 97% activation of homomultimeric Kir 3.2 over basal currents (Figure 7A,E). Note that stimulation of DAR-1 expressed in the absence of α_s led to markedly reduced (57 ± 8% over basal) channel activation (Figure 7B,E). Coexpression with various α_s mutants yielded varying degrees of channel activation. Consistent with its membrane localization, myr$^+$/palm$^+$ α_s also facilitated Kir 3.2 activation (Figure 7C,E). The polybasic, myr$^+$/polybasic, and 2palm α_s mediated activation but to a lesser extent, and the C3S α_s did not significantly activate Kir 3.2 (41 ± 12% over basal current levels) beyond the endogenous oocyte α_s background (Figure 7D,E).

Second, the ability of each α_s mutant to couple a coexpressed α_{2A}-adrenergic receptor (α_2-AR) to cAMP production was measured in transfected HEK293 cells (*1*). Agonist activation of α_2-AR stimulates cellular cAMP levels when coexpressed with α_s, but α_2-AR is unable to couple to endogenous α_s, thus providing a useful system for analyzing receptor coupling of transfected wild-type or mutant α_s subunits (*23*). In contrast, β_2-AR efficiently activates endogenous α_s, thus precluding the use of β_2-AR in transfected HEK293 cells to measure signaling by coexpressed α_s subunits. α_2-AR agonist stimulation resulted in a 2−6-fold elevation in cAMP levels when wild-type or N-terminal mutants of α_s were coexpressed with 2AR (Figure 8A). myr$^+$/palm$^+$ α_s was slightly less efficient than wt α_s (4-fold versus 6-fold) in coupling the α_2-AR to cAMP production while the other mutants consistently mediated cAMP stimulation only 2−3-fold over unstimulated levels (Figure 8A). The differing ability of α_s mutants to couple α_2-AR to cAMP production (Figure 8A) parallels results obtained assaying DAR-1 activation of Kir 3.2 channels in *Xenopus* oocytes (Figure 7).

Direct activation of the effector adenylyl cyclase, in the absence of GPCR stimulation, was assayed using α_sRC or each α_s mutant containing the activating RC mutation. In this assay, expression of α_sRC in HEK293 cells consistently raised cAMP levels more than 10-fold over unactivated wild-type α_s alone (not shown) (*1*). As expected, each N-terminal α_s mutant containing the RC mutation constitutively stimulated cAMP production (Figure 8B). Moreover, all mutants except myr$^+$/palm$^-$ α_s stimulated cAMP production 2−4-

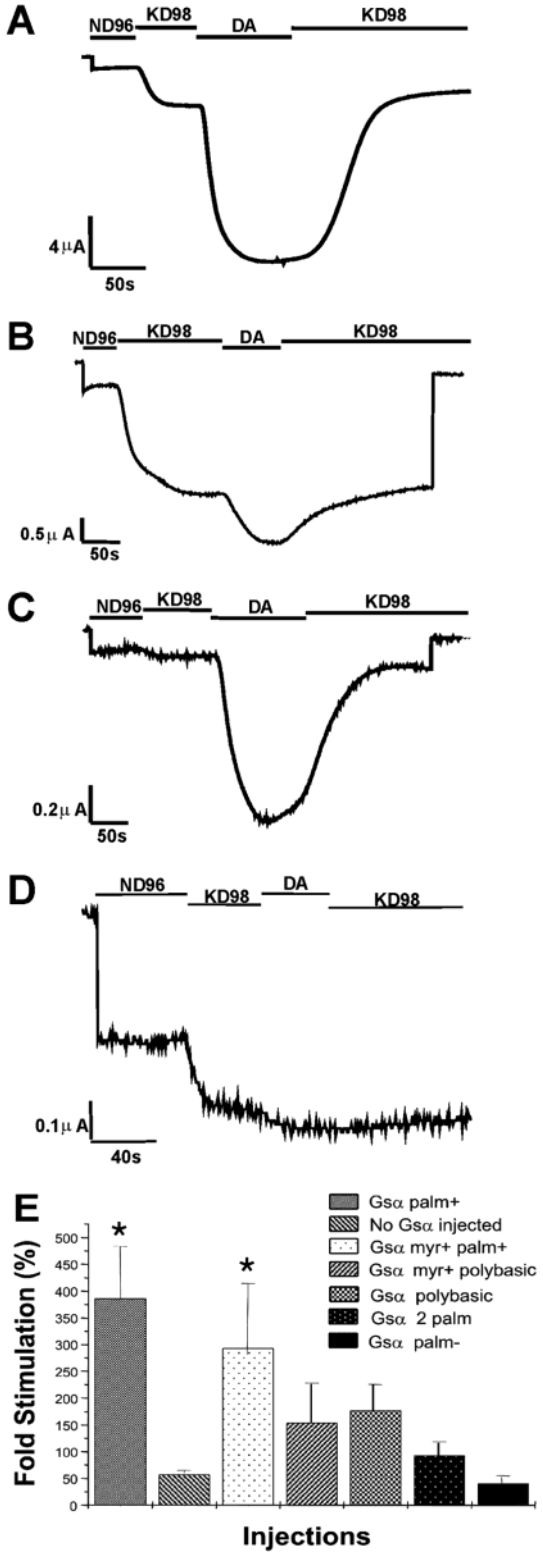

FIGURE 7: Stimulation of Kir 3.2 by DAR-1 requires membrane-associated α_s subunits. Oocytes were injected with cRNAs as described in Experimental Procedures. Parts A−D show representative traces of oocytes held at −80 mV. Stimulation by 1 μM dopamine of DAR-1 with (A) wild-type α_s (palm$^+$), (B) no exogenous α_s, (C) myr$^+$/palm$^+$ α_s, or (D) C3S α_s is shown. (E) Summary of results obtained for all mutants. Each of these experiments was reproduced at least four times in different oocytes. Data are presented as mean ± SEM for percent stimulation of activated currents over basal currents to control for variability in oocyte expression levels. Asterisks denote statistical difference between receptor expressed alone or with individual α_s variants ($p < 0.05$).

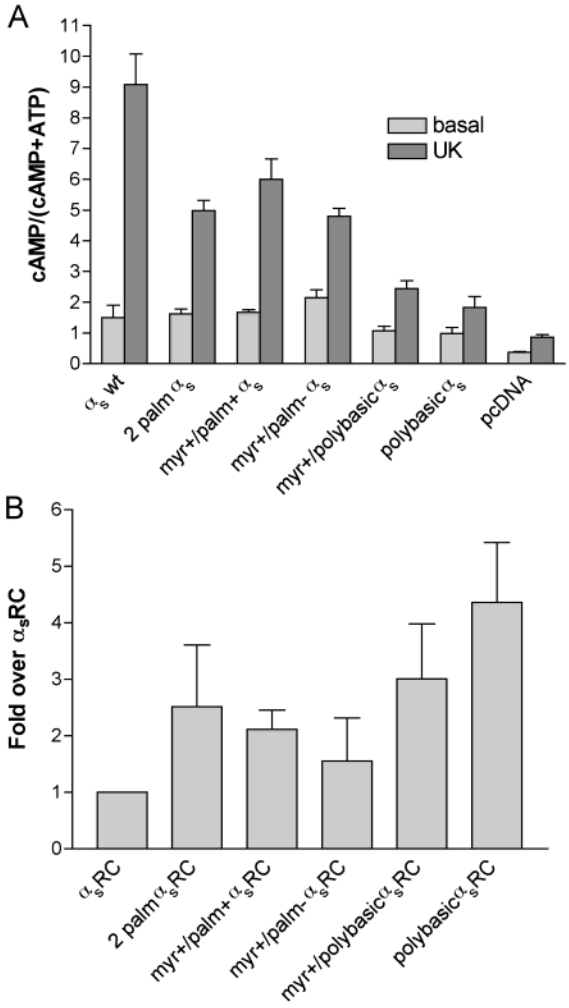

FIGURE 8: cAMP signaling by α_s mutants. (A) HEK293 cells were transfected with 500 ng of α_{2A}-AR-pCMV4, 200 ng of β_1-pCMV5, 100 ng of γ_2-pcDNAI, and 200 ng of pcDNA containing the indicated α_s mutant. Cells were treated with or without 10 μM UK-14304 for 45 min, and cAMP accumulation was measured as described in Experimental Procedures. Shown is a representative experiment assayed in triplicate. (B) HEK293 cells were transfected with 200 ng of pcDNA expression vectors for α_s or each N-terminal mutant of α_s containing the R201C activating mutation and 800 ng of pcDNA3, as indicated. The level of cAMP was determined and normalized to protein expression level as decribed in Experimental Procedures. Normalized cAMP produced in response to activated α_sR201C was arbitrarily set at 1. The results shown are the means ± SD for three experiments, each assayed in triplicate.

fold better than α_sRC (Figure 8B). Thus, α_s mutants that fail to translocate off the plasma membrane upon activation show an enhanced ability to raise cellular levels of cAMP.

DISCUSSION

Inside the cell, α_s can move reversibly from plasma membranes to cytoplasm in response to activation by GPCRs or activating mutations within the G protein itself. The results presented herein provide insight into the mechanism of this regulated translocation and highlight the importance of the unique N-terminus of α_s. Replacing the extreme N-terminus of α_s with alternate membrane targeting motifs resulted in mutant α_s subunits that were correctly targeted to plasma membranes but, in contrast to wild-type α_s, remained attached to plasma membranes after activation.

We used four different plasma membrane targeting motifs to replace the single N-terminal site of palmitoylation of α_s: (1) tandem myristoylation and palmitoylation ($myr^+/palm^+$), as found in G protein α subunits of the α_i subfamily; (2) dual palmitoylation (2palm), as found in α_q; (3) myristoylation followed by a polybasic motif (myr^+/polybasic), as found in c-src; and (4) a 20 amino acid sequence from GRK5 lacking any known site of lipid modification (polybasic) (*36*). An additional mutant, $myr^+/palm^-$ α_s, was poorly localized to plasma membranes, consistent with studies of other $myr^+/palm^-$ α subunits (*39*). However, the other four N-terminal mutants described above localized to plasma membranes as well as or better than wild-type α_s. However, critical differences were revealed between the N-terminal mutants and wild- type α_s when the subcellular localizations of activated forms were compared. α_sRC, containing the constitutively activating arginine 201 to cysteine mutation, shows a dramatic change in its localization. Whereas wild-type α_s is found at plasma membranes, activated α_sRC displays a pronounced shift to the cytoplasm, as assayed by immunofluorescence (*18*) (Figure 1A), and a substantial shift from a particulate to soluble cell fraction (*17*, *19*) (Figure 1B). In contrast, the introduction of the RC activating mutation into the N-terminal mutants had little or no effect on subcellular localization (Figures 4 and 5). The 2palm α_s displayed a small shift to the cytoplasm, as observed by both fractionation and immunofluorescence, upon RC mutational activation. Importantly, the RC activating mutation failed to induce a shift of the other N-terminal mutants to the cytoplasm (Figures 4 and 5). Activation-induced redistribution of α_s was also tested by acute activation of coexpressed β_2-AR. Agonist activation of β_2-AR induced no or small (polybasic α_s) changes in localization of the N-terminal α_s mutants, although wild-type α_s undergoes a rapid and pronounced redistribution from plasma membranes to cytoplasm (Figure 6 and Table 2) (*18*). These results with both mutational and GPCR-mediated activation of α_s indicate that the alternate membrane binding motifs can overcome the ability of wild-type α_s to redistribute from the plasma membrane.

α_s may be unique among G protein α subunits in its ability to translocate from plasma membranes to cytoplasm in response to activation. Activated forms of other G protein α subunits remain firmly attached to membranes (Figure 1), and rapid redistribution of other G protein α subunits in response to an activated GPCR has not been well described. Our results suggest that this difference between α_s and other G protein α subunits can be ascribed to differences in the extreme N-termini of the G protein α subunits. If unique sequences (other than the short N-terminus), signaling activities, or protein binding partners allow α_s to translocate from the plasma membrane in response to activation, the N-terminal mutants should retain this translocating activity. Instead, our results suggest that the extreme N-terminus containing the single palmitoylated cysteine is of critical importance. We propose, on the basis of these results, that other G protein α subunits display a weaker propensity for activation-induced release from membranes due to the presence of two rather than one covalently attached fatty acid. Whereas α_s appears to be modified by a single palmitate, other G protein α subunits contain two sites of palmitoylation (e.g., α_q) or tandem myristoylation and palmitoylation (e.g., α_i). Activation-induced depalmitoylation of α_s (*12*−*14*) correlates with its activation-induced redistribution (*18*); however, α_i and α_q also can undergo activation-induced depalmitoylation (*15*, *16*) yet fail to rapidly redistribute upon activation. Thus, the presence of more than one covalently attached fatty acid may decrease the likelihood that a G protein α subunit would be released from the PM after activation. Our results support this hypothesis. Taken together, the results presented here utilizing N-terminal mutants of α_s are consistent with the model that regulated cycles of acylation and deacylation constitute the underlying mechanism for observations of activation-induced subcellular redistribution of α_s (*6*, *18*).

Although the singly palmitoylated N-terminus of α_s appears to be important for allowing activation-induced redistribution of α_s, other differences among α subunits may contribute to differing abilities to translocate from plasma membranes to cytoplasm. In this regard, a singly palmitoylated α_z mutant did not redistribute from its plasma membrane location after GPCR stimulation (*39*). Thus, further studies of the importance of the extreme N-terminus of α_s will require the construction and analysis of chimeric α subunits in which portions of the N-terminus of α_i (or α_z) are replaced with corresponding sequences from α_s with the goal of creating an α_i that undergoes activation-induced redistribution.

Rodbell originally proposed the idea that certain G protein subunits could dissociate from the plasma membrane upon activation (*44*), and a number of studies, utilizing a variety of cell types, have supported and extended this theory. Agonist stimulation of Gs-coupled GPCRs in S49 cells (*17*, *21*) or mastocytoma P-185 cells (*20*) increased the fraction of cytosolic α_s, while activation of membrane preparations, from various cell types, by GPCR agonists or GTP analogues causes α_s to dissociate from membranes (*20*, *45*−*47*). β-AR activation in adipocytes (*48*) shifted α_s to a low-density membrane fraction. Moreover, a β-AR-induced shift of endogenous, stably transfected (*18*), or transiently transfected (this report) α_s from plasma membranes to cytoplasm has been observed by immunofluorescence microscopy of HEK 293 cells. A β-AR-induced redistribution of α_s has also been recently observed in live cells using a GFP-tagged α_s (*22*). Cholera toxin (CTX) ADP-ribosylates and activates α_s, and likewise, CTX treatment can induce a translocation of α_s from membranes to cytoplasm (*17*, *18*, *22*, *49*). Last, mutational activation of α_s results in a dramatic increase in cytosolic α_s in stably transfected S49 cyc- (*17*), MDCK (*19*), or HEK293 (*18*) cells. Strikingly, in all three cell types, greater than 80% of the stably expressed mutationally activated α_s is found in a cytosolic fraction, whereas less than 10% of stably expressed wild-type α_s is cytosolic. Although our results (*18*) (this report) show that transfected HEK293 cells provide a suitable system for analyzing localization differences between activated and wild-type α_s subunits, others have reported a lack of difference between transiently transfected wild-type and mutationally activated α_s in COS cells (*50*), suggesting that activation-induced redistribution of α_s may be difficult to detect in some cell systems.

Interestingly, α_q displays some propensity to change subcellular localization upon activation. A GFP-tagged form of α_qRC showed decreased localization at plasma membranes

and increased localization in the cytoplasm of transfected live cells, though no difference between wild-type α_q and α_qRC was found by fractionation (*30*). In agreement with those results, we found no difference between wild-type α_q and α_qRC by fractionation (Figure 1B), but we did observe, by immunofluorescence microscopy, a small but significant decrease in plasma membrane localization of α_qRC (Table 1). In addition, we observed an effect of the N-terminus of α_q when assayed in the context of α_s. The 2palm α_s displayed a small shift to the cytoplasm or soluble fraction, as observed by immunofluorescence (Table 2) and fractionation (Figure 4), upon RC mutational activation, consistent with the idea that α_q may have the ability to translocate off the plasma membrane upon activation. Furthermore, stimulation of the thyrotropin-releasing hormone (TRH) receptor has been observed to cause a redistribution of α_{11} (89% identical to α_q) from the plasma membrane into intracellular bodies (*51*, *52*). In contrast to α_s, agonist-induced redistribution of α_{11} required long-term agonist treatment (>2 h), and further stimulation (>4 h) led to loss of α_{11} from the cells (*51*, *52*). Further studies will more clearly define the similarities and differences between α_s and α_q in this regard.

One potential function for activation-induced redistribution of α_s is to desensitize α_s signaling by removing it from the plasma membrane where GPCRs and the effector, adenylyl cyclase, are located. Our results with mutationally activated α_s and its N-terminal mutants are consistent with such a role. α_sRC is found predominantly in the cytoplasm with a small fraction at the plasma membrane, and observations of rapid palmitate turnover suggest that α_sRC cycles between the plasma membrane and cytoplasm (*14*). N-Terminal mutants of α_s, containing the activating RC mutation, remain at the plasma membrane and, consistently, stimulate the production of cellular cAMP at levels 2−4-fold higher than α_sRC (Figure 8B). Thus, in this simple model, decreased plasma membrane localization of α_s leads to less cAMP signaling, while increased plasma membrane localization results in increased signaling. Studies utilizing α_s fused to a transmembrane tether or to the C-terminus of the β_2-AR also suggest that tighter membrane binding can result in higher levels of signaling. In membrane preparations of Sf9 cells, tet-α_s (tethered to membrane via a membrane spanning sequence) was activated by β_2-AR, as measured by GTPγS binding, to a greater degree compared to wild-type expressed α_s (*53*). In addition, a β_2-AR-α_s fusion protein more efficiently stimulated adenylyl cyclase compared to membranes containing normal β_2-AR and α_s (*54*). However, it is likely that other factors, in addition to strength of membrane binding, play roles in determining efficiency of adenylyl cyclase stimulation by α_s. These additional regulations may include localization to lipid raft domains and interactions with proteins other than adenylyl cyclase. Indeed, polybasic α_sRC displayed the highest level of cAMP stimulation (Figure 8B); it is unclear why this particular α_s mutant was better than the other plasma membrane localized α_s mutants (Figure 8B) in constitutive cAMP stimulation. Further analysis of the importance of activation-induced redistribution of α_s may require stable expression of the various N-terminal mutants in α_s-lacking *cyc*- cells.

In addition to regulating subcellular localization, changes in the palmitoylation status of α_s may regulate interaction with other proteins. Palmitoylated forms of α_z and α_i are refractory to GTPase stimulation by GAIP (Gα-interacting protein) and RGS4 (regulator of G-protein signaling 4) (*55*), suggesting that depalmitoylation may be necessary for α subunits, at least of the α_i subfamily, to be "turned off" by RGS proteins. Very recently, the first RGS protein, RGS-PX1, that interacts with α_s was identified (*56*). It will be important to determine whether this α_s/RGS-PX1 interaction is also regulated by palmitoylation/depalmitoylation. Palmitoylation of α_s may affect its interaction with other proteins. Depalmitoylation of α_s decreases its affinity for $\beta\gamma$ (*57*), and a myristoylated but nonpalmitoylated α_{i1} is deficient in coupling to a coexpressed GPCR (*58*). Depalmitoylation and/or membrane release of α_s could regulate interactions with tubulin; functional interactions with tubulin required the N-terminus of α_s (*59*). Thus, activation-induced depalmitoylation and redistribution may regulate the function of α_s in multiple ways.

Indeed, we found that the N-terminal α_s mutants varied in their ability to couple GPCRs to effector stimulation, as measured in two different assays. Although all of the mutants couple α_2-AR to cAMP production in HEK293 cells or DAR-1 receptors to Kir 3.2 channel activation in oocytes, wt α_s consistently mediated a higher fold stimulation compared to the mutants. Regions of the N-termini of Gα have been implicated as important sites for mediating coupling to GPCRs (*60*). It is not clear, however, whether the N-termini of Gα affect interactions with GPCRs through interactions with $\beta\gamma$, effects on Gα C-termini (a well-described site for GPCR interactions), direct interactions with GPCRs, or specific roles for lipid modifications. Covalently attached myristate and/or palmitate could promote or inhibit interactions with different GPCRs via direct lipid−protein interactions or could serve to help orient the G protein heterotrimer. Our α_s mutants do not distinguish between these possibilities, but they do highlight a potential role for Gα N-termini in GPCR coupling.

The N-terminal mutants of α_s described here further define the differences between agonist-induced trafficking of β_2-AR and α_s. Our previous results demonstrated that, under conditions in which β_2-AR internalization is blocked, α_s redistribution is unaffected (*18*). Another report demonstrated temporal and spatial separation of activated TRH receptors and slowly internalizing α_{11} (*52*). Now we further separate β_2-AR endocytosis and α_s translocation by showing that N-terminal mutants of α_s remain at the plasma membrane even though β_2-AR is efficiently internalizing (Figure 6). This observation provides further evidence that α_s may not accompany the β_2-AR during membrane vesicle trafficking. Although it is clear that a large portion of α_s is translocated to the cytoplasm upon receptor activation, a significant amount remains associated with the plasma membrane fraction (Figure 6) (*18*). This is consistent with a recent report of more stable receptor−Gs interactions (*61*). Further studies of differential receptor−G protein trafficking are required to determine where their itineraries become separate. Interestingly, the α_s-specific RGS-PX1 has been localized to endosomes (*56*), suggesting that this could be a site for "turning off" (by GTP hydrolysis) α_s and/or reassembling a G_s heterotrimer (*62*).

Last, our results with creating a myristoylated α_s help to explain why α_s is not normally myristoylated even though it contains a glycine at position 2. A majority of myristoy-

lated proteins contain a serine or threonine at position 6 (*10*, *63*), and it appears that, other than the invariant glycine, this is the most critical position in terms of a consensus sequence for myristoylation. Indeed α_i, α_o, α_z, and α_t all have a serine a position 6. α_s, on the other hand, has an asparagine at this position. When this asparagine was changed to a serine (α_s-N6S), α_s remained nonmyristoylated (Figure 3), confirming an earlier report (*64*). However, an additional change of leucine 4 to threonine and glycine 5 to leucine (Figure 2), to exactly match the first six amino acids of α_{i1}, allowed myristoylation of this α_s mutant ($myr^+/palm^+$). More than 100 myristoylated proteins have been identified (*63*), and a variety of amino acids can be accommodated at positions 4 and 5. Indeed, a search of the N-terminal sequences of myristoylated proteins (*10*, *63*) shows that leucine at position 4 is tolerated, as is glycine at position 5. However, so far there are no examples of myristoylated proteins containing both leucine 4 and glycine 5, consistent with the inability of wild-type or N6S α_s to be modified by myristate. Thus, several amino acids appear to play a role in preventing the myristoylation of α_s.

The N-termini of Gα are regions of great diversity in terms of amino acid sequence, length of the extension, and types and combinations of lipid modifications present. It seems likely that such differences will contribute to different signaling functions and specificity. The work presented here highlights the unique N-terminus of α_s and its role in activation-induced translocation of α_s.

ACKNOWLEDGMENT

The authors thank Dr. Balasamy Thiyagarajan for kind assistance in statistical analysis of data, Steven Luke for excellent and dedicated assistance with confocal microscopy, Debra Garlin for technical assistance, Dr. Alexey Pronin for advice on using the GRK5 membrane localization sequence, and Drs. Jeff Benovic and Catherine Chen for critical reading of the manuscript.

SUPPORTING INFORMATION AVAILABLE

One figure showing subcellular localization of GRK5-GFP and GRK2-GFP with α_s by confocal immunofluorescence microscopy. This material is available free of charge via the Internet at http://pubs.acs.org.

REFERENCES

1. Evanko, D. S., Thiyagarajan, M. M., and Wedegaertner, P. B. (2000) *J. Biol. Chem. 275*, 1327−1336.
2. Evanko, D. S., Thiyagarajan, M. M., Siderovski, D. P., and Wedegaertner, P. B. (2001) *J. Biol. Chem. 276*, 23945−23953.
3. Wang, Y., Windh, R. T., Chen, C. A., and Manning, D. R. (1999) *J. Biol. Chem. 274*, 37435−37442.
4. Fishburn, C. S., Herzmark, P., Morales, J., and Bourne, H. R. (1999) *J. Biol. Chem. 274*, 18793−18800.
5. Fishburn, C. S., Pollitt, S. K., and Bourne, H. R. (2000) *Proc. Natl. Acad. Sci. U.S.A. 97*, 1085−1090.
6. Wedegaertner, P. B. (1998) *Biol. Signals Recept. 7*, 125−135.
7. Dunphy, J. T., and Linder, M. E. (1998) *Biochim. Biophys. Acta 1436*, 245−261.
8. Chen, C. A., and Manning, D. R. (2001) *Oncogene 20*, 1643−1652.
9. Peitzsch, R. M., and McLaughlin, S. (1993) *Biochemistry 32*, 10436−10443.
10. Resh, M. D. (1999) *Biochim. Biophys. Acta 1451*, 1−16.
11. Wedegaertner, P. B., Wilson, P. T., and Bourne, H. R. (1995) *J. Biol. Chem. 270*, 503−506.
12. Degtyarev, M. Y., Spiegel, A. M., and Jones, T. L. (1993) *J. Biol. Chem. 268*, 23769−23772.
13. Mumby, S. M., Kleuss, C., and Gilman, A. G. (1994) *Proc. Natl. Acad. Sci. U.S.A. 91*, 2800−2804.
14. Wedegaertner, P. B., and Bourne, H. R. (1994) *Cell 77*, 1063−1070.
15. Bhamre, S., Wang, H. Y., and Friedman, E. (1998) *J. Pharmacol. Exp. Ther. 286*, 1482−1489.
16. Chen, C. A., and Manning, D. R. (2000) *J. Biol. Chem. 275*, 23516−23522.
17. Levis, M. J., and Bourne, H. R. (1992) *J. Cell Biol. 119*, 1297−1307.
18. Wedegaertner, P. B., Bourne, H. R., and von Zastrow, M. (1996) *Mol. Biol. Cell 7*, 1225−1233.
19. Hansen, S. H., and Casanova, J. E. (1994) *J. Cell Biol. 126*, 677−687.
20. Negishi, M., Hashimoto, H., and Ichikawa, A. (1992) *J. Biol. Chem. 267*, 2364−2369.
21. Ransnas, L. A., Svoboda, P., Jasper, J. R., and Insel, P. A. (1989) *Proc. Natl. Acad. Sci. U.S.A. 86*, 7900−7903.
22. Yu, J.-Z., and Rasenick, M. M. (2002) *Mol. Pharmacol. 61*, 352−359.
23. Wedegaertner, P. B., Chu, D. H., Wilson, P. T., Levis, M. J., and Bourne, H. R. (1993) *J. Biol. Chem. 268*, 25001−25008.
24. Pace, A. M., Faure, M., and Bourne, H. R. (1995) *Mol. Biol. Cell 6*, 1685−1695.
25. Faure, M., Voyno-Yasenetskaya, T. A., and Bourne, H. R. (1994) *J. Biol. Chem. 269*, 7851−7854.
26. Woolson, R. F. (1987) *Statistical Methods for the Analysis of Biomedical Data*, John Wiley and Sons, New York.
27. Barak, L. S., Ferguson, S. S., Zhang, J., and Caron, M. G. (1997) *J. Biol. Chem. 272*, 27497−27500.
28. Weerapura, M., Nattel, S., Courtemanche, M., Doern, D., Ethier, N., and Hebert, T. (2000) *J. Physiol. 526*, 265−278.
29. Robillard, L., Ethier, N., Lachance, M., and Hebert, T. E. (2000) *Cell. Signal. 12*, 673−682.
30. Hughes, T. E., Zhang, H., Logothetis, D. E., and Berlot, C. H. (2001) *J. Biol. Chem. 276*, 4227−4235.
31. Silverman, L., and Resh, M. D. (1992) *J. Cell Biol. 119*, 415−425.
32. Sigal, C. T., Zhou, W., Buser, C. A., McLaughlin, S., and Resh, M. D. (1994) *Proc. Natl. Acad. Sci. U.S.A. 91*, 12253−12257.
33. McCabe, J. B., and Berthiaume, L. G. (1999) *Mol. Biol. Cell 10*, 3771−3786.
34. Kostenis, E., Degtyarev, M. Y., Conklin, B. R., and Wess, J. (1997) *J. Biol. Chem. 272*, 19107−19110.
35. Hepler, J. R., Biddlecome, G. H., Kleuss, C., Camp, L. A., Hofmann, S. L., Ross, E. M., and Gilman, A. G. (1996) *J. Biol. Chem. 271*, 496−504.
36. Pronin, A. N., Carman, C. V., and Benovic, J. L. (1998) *J. Biol. Chem. 273*, 31510−31518.
37. Wilson, P. T., and Bourne, H. R. (1995) *J. Biol. Chem. 270*, 9667−9675.
38. Barak, L. S., Warabi, K., Feng, X., Caron, M. G., and Kwatra, M. M. (1999) *J. Biol. Chem. 274*, 7565−7569.
39. Morales, J., Fishburn, C. S., Wilson, P. T., and Bourne, H. R. (1998) *Mol. Biol. Cell 9*, 1−14.
40. von Zastrow, M., and Kobilka, B. K. (1992) *J. Biol. Chem. 267*, 3530−3538.
41. von Zastrow, M., and Kobilka, B. K. (1994) *J. Biol. Chem. 269*, 18448−18452.
42. Ng, G. Y., Bertrand, S., Sullivan, R., Ethier, N., Wang, J., Yergey, J., Belley, M., Trimble, L., Bateman, K., Alder, L., Smith, A., McKernan, R., Metters, K., O'Neill, G. P., Lacaille, J. C., and Hebert, T. E. (2001) *Mol. Pharmacol. 59*, 144−152.
43. Fidler-Lim, N., Dascal, N., Labarca, C., Davidson, N., and Lester, H. A. (1995) *J. Gen. Physiol. 105*, 421−439.
44. Rodbell, M. (1985) *Trends Biochem. Sci. 10*, 461−464.
45. Ransnas, L. A., Jasper, J. R., Leiber, D., and Insel, P. A. (1992) *Biochem. J. 283*, 519−524.
46. Milligan, G., and Unson, C. G. (1989) *Biochem. J. 260*, 837−841.
47. Witte, K., Schnecko, A., and Lemmer, B. (1999) *Biochem. Pharmacol. 57*, 539−543.
48. Haraguchi, K., and Rodbell, M. (1990) *Proc. Natl. Acad. Sci. U.S.A. 87*, 1208−1212.
49. Lynch, C. J., Morbach, L., Blackmore, P. F., and Exton, J. H. (1986) *FEBS Lett. 200*, 333−336.

50. Huang, C., Duncan, J. A., Gilman, A. G., and Mumby, S. M. (1999) *Proc. Natl. Acad. Sci. U.S.A. 96*, 412−417.
51. Drmota, T., Novotny, J., Kim, G. D., Eidne, K. A., Milligan, G., and Svoboda, P. (1998) *J. Biol. Chem. 273*, 21699−21707.
52. Drmota, T., Novotny, J., Gould, G. W., Svoboda, P., and Milligan, G. (1999) *Biochem. J. 340*, 529−538.
53. Lee, T. W., Seifert, R., Guan, X., and Kobilka, B. K. (1999) *Biochemistry 38*, 13801−13809.
54. Seifert, R., Wenzel-Seifert, K., Gether, U., Lam, V. T., and Kobilka, B. K. (1999) *Eur. J. Biochem. 260*, 661−666.
55. Tu, Y., Wang, J., and Ross, E. M. (1997) *Science 278*, 1132−1135.
56. Zheng, B., Ma, Y.-C., Ostrom, R. S., Lavoie, C., Gill, G. N., Insel, P. A., Huang, X.-Y., and Farquhar, M. G. (2001) *Science 294*, 1939−1942.
57. Iiri, T., Backlund, P. S., Jr., Jones, T. L., Wedegaertner, P. B., and Bourne, H. R. (1996) *Proc. Natl. Acad. Sci. U.S.A. 93*, 14592−14597.
58. Wise, A., Grassie, M. A., Parenti, M., Lee, M., Rees, S., and Milligan, G. (1997) *Biochemistry 36*, 10620−10629.
59. Popova, J. S., Johnson, G. L., and Rasenick, M. M. (1994) *J. Biol. Chem. 269*, 21748−21754.
60. Hamm, H. E. (1998) *J. Biol. Chem. 273*, 669−672.
61. Lachance, M., Ethier, N., Wolbring, G., Schnetkamp, P. P., and Hebert, T. E. (1999) *Cell. Signal. 11*, 523−33.
62. von Zastrow, M., and Mostov, K. (2001) *Science 294*, 1845−1847.
63. Boutin, J. A. (1997) *Cell. Signal. 9*, 15−35.
64. Mumby, S. M., and Linder, M. E. (1994) *Methods Enzymol. 237*, 254−268.

BI025533U